Conference Proceedings of the Society for Experimental Mechanics Series

Randy Mayes · Daniel Rixen · Matt Allen *Editors*

Topics in Experimental Dynamic Substructuring, Volume 2

Proceedings of the 31st IMAC, A Conference on Structural Dynamics, 2013

SEM

Springer

Randy Mayes • Daniel Rixen • Matt Allen
Editors

Topics in Experimental Dynamic Substructuring, Volume 2

Proceedings of the 31st IMAC, A Conference on Structural Dynamics, 2013

Springer

Editors
Randy Mayes
Sandia National Laboratories
Albuquerque, NM, USA

Matt Allen
Engineering Physics Department
University of Wisconsin Madison
Madison, WI, USA

Daniel Rixen
Department of Precision and Microsystems Engineering
Delft University of Technology
Delft, Netherlands

ISSN 2191-5644 ISSN 2191-5652 (electronic)
ISBN 978-1-4614-6539-3 ISBN 978-1-4614-6540-9 (eBook)
DOI 10.1007/978-1-4614-6540-9
Springer New York Heidelberg Dordrecht London

Library of Congress Control Number: 2013939185

Printed on acid-free paper

Springer is part of Springer Science+Business Media (www.springer.com)

Preface

Topics in Experimental Dynamic Substructuring, Volume 2: Proceedings of the 31st IMAC, A Conference on Structural Dynamics, 2013 represents one of the seven volumes of technical papers presented at the 31st IMAC, a conference and exposition on structural dynamics, 2013, organized by the Society for Experimental Mechanics and held in Garden Grove, California, from February 11 to 14, 2013. The full proceedings also include volumes on nonlinear dynamics; dynamics of bridges; dynamics of civil structures; model validation and uncertainty quantification; special topics in structural dynamics; and modal analysis.

Each collection presents early findings from experimental and computational investigations on an important area within structural dynamics. Substructuring is one of these areas.

Substructuring is a general paradigm in engineering dynamics where a complicated system is analyzed by considering the dynamic interactions between subcomponents. In numerical simulations, substructuring allows one to reduce the complexity of parts of the system in order to construct a computationally efficient model of the assembled system. A subcomponent model can also be derived experimentally, allowing one to predict the dynamic behavior of an assembly by combining experimentally and/or analytically derived models. This can be advantageous for subcomponents that are expensive or difficult to model analytically. Substructuring can also be used to couple numerical simulation with real-time testing of components. Such approaches are known as hardware-in-the-loop or hybrid testing.

Whether experimental or numerical, all substructuring approaches have a common basis, namely the equilibrium of the substructures under the action of the applied and interface forces and the compatibility of displacements at the interfaces of the subcomponents. Experimental substructuring requires special care in the way the measurements are obtained and processed in order to assure that measurement inaccuracies and noise do not invalidate the results. In numerical approaches, the fundamental quest is the efficient computation of reduced order models describing the substructure's dynamic motion. For hardware-in-the-loop applications difficulties include the fast computation of the numerical components and the proper sensing and actuation of the hardware component. Recent advances in experimental techniques, sensor/actuator technologies, novel numerical methods, and parallel computing have rekindled interest in substructuring in recent years, leading to new insights and improved experimental and analytical techniques.

The organizers would like to thank the authors, presenters, session organizers, and session chairs for their participation in this track.

Albuquerque, NM, USA — Randy Mayes
Delft, Netherlands — Daniel Rixen
Madison, WI, USA — Matt Allen

Contents

Chapter 1
Integrating Biodynamic Measurements in Frequency-Based Substructuring to Study Human-Structure Interaction

Sébastien Perrier, Yvan Champoux, and Jean-Marc Drouet

Abstract The mechanical behavior of the human body has long been characterized using biodynamic measurements on various human body parts in several positions and postures. Generally, these measurements are gathered as close as possible to the skin-mechanical structure interface for best results understanding how the body reacts when in contact with a vibrating structure. Substructuring methods have been widely used on mechanical structures to study and improve the dynamic behavior of complex assemblies. In the case of interactions between a human body and a vibrating structure, the dynamics involved in the structure alone is as important as the dynamics of the human body. Thus, the use of Frequency-Based Substructuring (FBS) to combine biodynamic measurements with the structure's dynamic behavior is essential to understanding the vibration transmission phenomena in this complex assembly.

This article presents the advantages of this approach as well as the challenges when performing FBS between a mechanical structure and biodynamic measurements. The study focuses on a vibrating handlebar in conjunction with 3 different holding positions of the hand-arm system. The FBS assemblies are gathered and the results are compared with experimental measurements on the entire assembled structure for each position over a frequency range between 1 and 100 Hz.

Keywords Biodynamics • Substructuring • Human-structure interaction • Experimental measurements • Structural dynamics

1.1 Introduction

The mechanical behavior of the human body under vibration has long been characterized and studied in the context of health and safety, as well as in the context of dynamic comfort evaluation. Among them, whole-body vibration and hand-transmitted vibration have been studied the most in order to minimize the undesirable effects of vibration [1–19]. Hand-transmitted vibration is of great interest since the hands are highly sensitive in capturing vibration discomfort and high levels of hand vibration can even be detrimental to overall health.

The characterization of hand-transmitted vibration (HTV) depends on several parameters such as vibration frequency and magnitudes, axis of vibration, coupling forces, frequency weighting, and others. For example in ISO-5349 [13], which documents the measurement, the dose–response relationship, and the weighting filter for assessment of HTV, the current weighting function proposed significantly suppresses the magnitude of vibration at frequencies above 100 Hz. The dynamic response behavior of the hand-arm system can be described as *through-the-hand-arm* and *to-the-hand* response functions. The *through-the-hand-arm* response function describes the transmission of vibration as the ratio of the motion magnitude at a specific segment of the hand-arm to that at the hand-handle interface. The biodynamic response in terms of the *to-the-hand* function relates the vibration in the vicinity of the hand to the force at the driving point [7]. The *to-the-hand* dynamic response behavior is the one to use when studying humans in contact with vibrating structures. This biodynamic response behavior has been extensively investigated, but the majority of the studies are based upon either the absorbed power or the driving point mechanical impedance Z (DPMI). These two expressions are relatively similar. The DPMI is computed from

S. Perrier (✉) • Y. Champoux • J.-M. Drouet
Department of Mechanical Engineering, VélUS, Université de Sherbrooke, 2500 boul. de l'Université, Sherbrooke, QC, Canada J1K 2R1
e-mail: Sebastien.Perrier@USherbrooke.ca

R. Mayes et al. (eds.), *Topics in Experimental Dynamic Substructuring, Volume 2: Proceedings of the 31st IMAC, A Conference on Structural Dynamics, 2013*, Conference Proceedings of the Society for Experimental Mechanics Series 36,
DOI 10.1007/978-1-4614-6540-9_1,

the force F – velocity v relationship at the driving point, as described in Eq. (1.1), and the vibration power at the driving point is computed from the parameters used in calculating the DPMI, as described in Eq. (1.2).

$$Z(j\omega) = \frac{F(j\omega)}{v(j\omega)} \tag{1.1}$$

$$P(\omega) = \mathrm{Re}[Z(j\omega)]\,|v(j\omega)|^2 \tag{1.2}$$

where v is the root-mean-square value of the velocity at the same frequency.

The biodynamic response characteristics of the human hand-arm have been measured on human subjects under carefully controlled conditions to control several parameters such as posture, hand position, type of excitation, excitation direction, push and grip forces [2–6]. Nonetheless, considerable differences are known to exist in the measured data reported by investigators. These differences have been partially attributed to variations in intrinsic and extrinsic variables, test conditions, methodologies employed in the various studies [1], and the dynamic behavior of the handle itself [8, 15].

With difficulties to obtain repetitive measurements involving representative human-subject samples and test conditions due to inter- and intrasubject variabilities, biodynamic models of the hand and arm have been proposed to characterize vibration amplitude and power flow in the coupled hand, structure, and workpiece system. The majority of the reported models are mechanical models that comprise lumped mass, stiffness, and damping elements in which the lumped parameter values are identified upon the curve fitting of the measured data.

The models, therefore, do not adequately represent the biomechanical properties of the human hand and arm [7]. Furthermore, the models characterize the uncoupled biodynamic behavior of the hand and arm along the three independent orthogonal axes of vibration. All the models thus neglect to consider the dynamic coupling effects of the hand and arm.

Owing to the complex nature of the structure vibration and coupled hand-structure system dynamics, the approach developed in this work is to consider the hand-arm system as a "black box". Its dynamic response with measured DPMI can be described, and these characteristics assembled with those of the structure by a substructuring method to develop a coupling model for the study of human–structure interactions.

Substructuring methods have become a focus of research in structural dynamics [20–30] and have been used on mechanical structures to study and improve the dynamic behavior of complex assemblies. Whereas knowledge of the interactions between structure assemblies has been a major concern in mechanical engineering since the 1960s, studies of human–structure interactions in mechanics are sparsely documented in comparison.

To the authors' knowledge, the first attempt to study a substructuring coupling that involves both the human body and a mechanical structure was made by the authors themselves [31]. No human-structure interactions using the Frequency-Based Substructuring (FBS) method have been explored since that time. In contact with a human body part, the dynamic behavior of a lightweight structure changes radically from its original uncoupled condition. Therefore, the use of FBS to combine biodynamic measurements with the structure's dynamic behavior is essential to understand vibration transmission phenomena.

In this work, we present the advantages of this approach as well as the challenges when performing FBS using computed characteristics of the mechanical structure and biodynamic measurements. The FBS method allows coupling between substructures through consideration of their interface set only [26]. This is a major advantage in linking a mechanical structure with the human body where only interface measurements can be gathered. The study focuses on the hand-arm in conjunction with a vibrating structure in 3 different positions. Although the human body is not linear, mechanical coupling using the FBS method can be used with the hand-arm system by controlling various parameters [31]. Each substructure is characterized in the frequency range [1, 100] Hz. The mechanical structure is characterized by the mechanical mobility Frequency Response Function (FRF) using a Finite Elements model and the hand-arm by measured mechanical impedance FRF. Finite Elements (FE) are used to characterize the mechanical structure since all the mechanical information, as well as the translational and rotational degrees of freedom, are intrinsically available. The hybrid FBS assemblies are then gathered and the results are compared with experimental measurements over the entire assembled structure for each position.

1.2 Methods

The methods used in this paper to join the human hand-arm with a mechanical structure include the generalized frequency domain substructure synthesis presented in [26]. This well-known method, also referred to as FBS (Frequency-Based Substructuring), combines the response FRF data of each substructure to analyze the dynamics of a complex assembled structure. It enables substructures to be coupled by taking into account the characteristics of the interface nodes only. It can

also utilize experimentally derived data effectively in combination with finite element results. This method is based on an implicit statement of the force and velocity continuity considerations at the connection nodes. It leads to the mathematical expression for the FRF coupling of two substructures in terms of mobility Y (velocity/force) shown in Eq. (1.3) where: a and b identify the two substructures involved; A is the set of internal degrees of freedom in substructure a; I is the interface contact set between substructures a and b; and B is the set of internal degrees of freedom in substructure b.

$$\begin{bmatrix} \mathbf{Y}_{AA} & \mathbf{Y}_{AI} & \mathbf{Y}_{AB} \\ \mathbf{Y}_{IA} & \mathbf{Y}_{II} & \mathbf{Y}_{IB} \\ \mathbf{Y}_{BA} & \mathbf{Y}_{BI} & \mathbf{Y}_{BB} \end{bmatrix}^{ab} = \begin{bmatrix} \mathbf{Y}^a_{AA} & \mathbf{Y}^a_{AI} & 0 \\ \mathbf{Y}^a_{IA} & \mathbf{Y}^a_{II} & 0 \\ 0 & 0 & \mathbf{Y}^b_{BB} \end{bmatrix} - \begin{Bmatrix} \mathbf{Y}^a_{AI} \\ \mathbf{Y}^a_{II} \\ -\mathbf{Y}^b_{BI} \end{Bmatrix} \left[\mathbf{Y}^a_{II} + \mathbf{Y}^b_{II}\right]^{-1} \begin{Bmatrix} \mathbf{Y}^a_{IA} \\ \mathbf{Y}^a_{II} \\ -\mathbf{Y}^b_{IB} \end{Bmatrix}^{\mathrm{T}} \tag{1.3}$$

Substructures a and b represent the mechanical structure and the hand-arm, respectively. The coupling process using the FBS method is achieved by computing the mechanical structure mobility characteristics from the FE model and by measuring the impedance at the hands. These characteristics are assembled through Eq. (1.3) to predict the assembly's dynamic behavior. The mobility characteristics of the assembly are then compared with the measured mobility characteristics of the mechanical structure in contact with both hands. For this study, only interface data can be gathered for the hand-arm system, and therefore the equation can be simplified as shown in Eq. (1.4).

$$\begin{bmatrix} \mathbf{Y}_{AA} & \mathbf{Y}_{AI} \\ \mathbf{Y}_{IA} & \mathbf{Y}_{II} \end{bmatrix}^{ab} = \begin{bmatrix} \mathbf{Y}^a_{AA} & \mathbf{Y}^a_{AI} \\ \mathbf{Y}^a_{IA} & \mathbf{Y}^a_{II} \end{bmatrix} - \begin{Bmatrix} \mathbf{Y}^a_{AI} \\ \mathbf{Y}^a_{II} \end{Bmatrix} \left[\mathbf{Y}^a_{II} + \mathbf{Y}^b_{II}\right]^{-1} \begin{Bmatrix} \mathbf{Y}^a_{IA} \\ \mathbf{Y}^a_{II} \end{Bmatrix}^{\mathrm{T}} \tag{1.4}$$

Since the measurements of the mobility characteristics are made on the mechanical structure in contact with both hands, we are focusing only on the mechanical mobility determined by an excitation force applied at the internal set A for the substructure a and a velocity response at the interface set I.

$$\left[\mathbf{Y}^{ab}_{IA}\right] = \left[\mathbf{Y}^a_{IA}\right] - \left[\mathbf{Y}^a_{II}\right]\left[\mathbf{Y}^a_{II} + \mathbf{Y}^b_{II}\right]^{-1}\left[\mathbf{Y}^a_{IA}\right] \tag{1.5}$$

Equation (1.5) can be developed to reveal the left and right hands interface points, respectively, $I1$ and $I2$.

$$\begin{bmatrix} \mathbf{Y}^{ab}_{I1A} \\ \mathbf{Y}^{ab}_{I2A} \end{bmatrix} = \begin{bmatrix} \mathbf{Y}^a_{I1A} \\ \mathbf{Y}^a_{I2A} \end{bmatrix} - \begin{bmatrix} \mathbf{Y}^a_{I1I1} & \mathbf{Y}^a_{I1I2} \\ \mathbf{Y}^a_{I2I1} & \mathbf{Y}^a_{I2I2} \end{bmatrix} \left[\begin{bmatrix} \mathbf{Y}^a_{I1I1} & \mathbf{Y}^a_{I1I2} \\ \mathbf{Y}^a_{I2I1} & \mathbf{Y}^a_{I2I2} \end{bmatrix} + \begin{bmatrix} \mathbf{Y}^b_{I1I1} & \mathbf{Y}^b_{I1I2} \\ \mathbf{Y}^b_{I2I1} & \mathbf{Y}^b_{I2I2} \end{bmatrix}\right]^{-1} \begin{bmatrix} \mathbf{Y}^a_{I1A} \\ \mathbf{Y}^a_{I2A} \end{bmatrix} \tag{1.6}$$

Furthermore, assumption is made that left and right hands are dynamically independent.

$$\begin{bmatrix} \mathbf{Y}^{ab}_{I1A} \\ \mathbf{Y}^{ab}_{I2A} \end{bmatrix} = \begin{bmatrix} \mathbf{Y}^a_{I1A} \\ \mathbf{Y}^a_{I2A} \end{bmatrix} - \begin{bmatrix} \mathbf{Y}^a_{I1I1} & \mathbf{Y}^a_{I1I2} \\ \mathbf{Y}^a_{I2I1} & \mathbf{Y}^a_{I2I2} \end{bmatrix} \left[\begin{bmatrix} \mathbf{Y}^a_{I1I1} & \mathbf{Y}^a_{I1I2} \\ \mathbf{Y}^a_{I2I1} & \mathbf{Y}^a_{I2I2} \end{bmatrix} + \begin{bmatrix} \mathbf{Y}^b_{I1I1} & 0 \\ 0 & \mathbf{Y}^b_{I2I2} \end{bmatrix}\right]^{-1} \begin{bmatrix} \mathbf{Y}^a_{I1A} \\ \mathbf{Y}^a_{I2A} \end{bmatrix} \tag{1.7}$$

1.2.1 Target Measurements

These measurements are used to evaluate the accuracy of the FBS prediction for the mechanical structure coupled with both hands (Eq. (1.7)). The mechanical structure is an aluminum assembly composed of a handlebar, a stem and a support. Figure 1.1 shows the structure installed on an excitation device used to gather target measurements with both hands on the structure. This excitation device is a hydraulic excitation system able to handle important loads and designed to produce a vertical excitation. Only the vertical Z-axis is presented in this paper.

To get the mobility of this assembly (structure with hands on it), the excitation is characterized using a six degrees of freedom (DOFs) forces/moments sensor (AMTI MC3A-500) installed between the excitation device and the support, and an accelerometer is fixed to the handlebar as close as possible to the hands. The velocity is obtained by integrating the acceleration in the frequency domain. A vibration signal reproducing the dynamic characteristics of a road is provided to the excitation system [32]. The acquisition system is a LMS SCADAS Recorder using Test.Lab 12A software.

Three postures of the hand-arm leaning on the structure are tested (Fig. 1.2). Each of them requires that the arms be kept straight. For each posture, the subject is asked to hold the handle without applying any grip force, just leaning on the structure. The push force applied by the subject on the structure is measured to control the posture during acquisition. The subject is asked to maintain a constant push force during the test using the DC values displayed by the 6DOFs forces/moments sensor in the X and Z axes. For each posture, the DC values along X and Z axes are recorded for further use during the measurement of the hand-arm mechanical impedance.

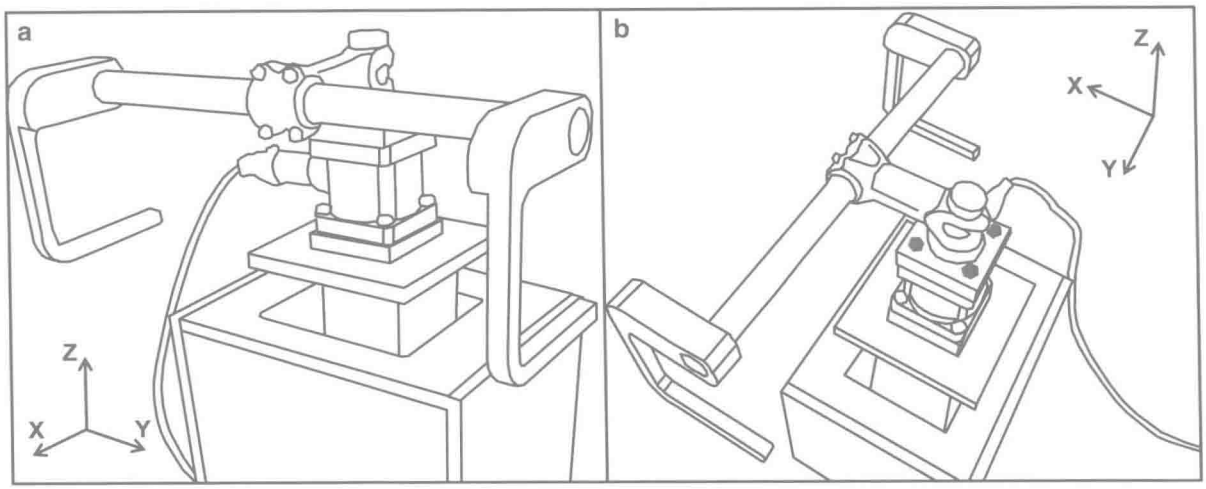

Fig. 1.1 Mechanical assembly with the 6DOFs forces/moments sensor installed on the excitation device. (**a**) *Front view*, (**b**) *Top view*

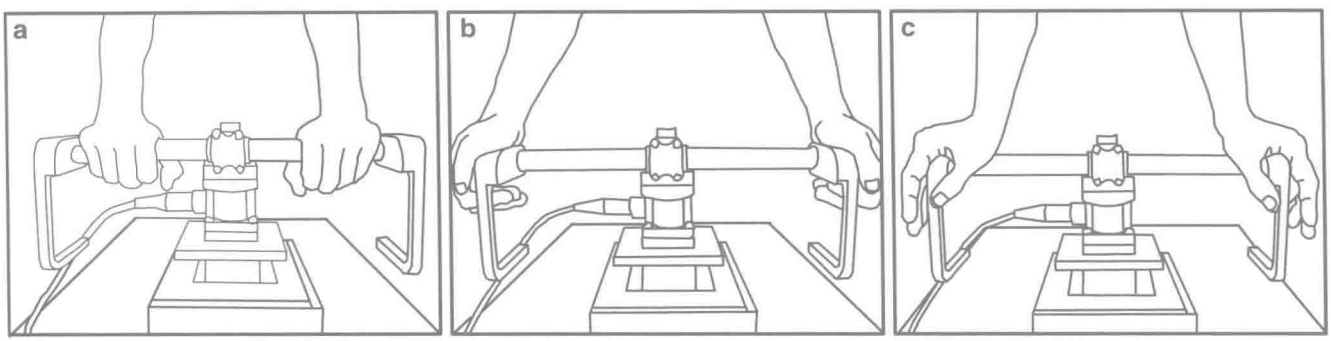

Fig. 1.2 Three test postures for the hands on the mechanical assembly. (**a**) Posture with DC values X: 10 N and Z: −70 N. (**b**) Posture with DC values X: 15 N and Z: −85 N. (**c**) Posture with DC values X: 25 N and Z: −105 N

1.2.2 Hand-Arm Mechanical Impedance

In Eq. (1.7), ${\boldsymbol{Y}_{111}}^{b}$ corresponds to the matrix mobility for the left hand-arm system and ${\boldsymbol{Y}_{212}}^{b}$ corresponds to the matrix mobility for the right hand-arm system. In these two matrices, only the term corresponding to an excitation and response along the vertical Z-axis is retained.

Typically, the dynamic characteristics of the hand-arm are in the form of mechanical impedance. For this reason and in this study, the hand-arm is characterized in terms of measured impedance. Theoretically, the mobility also known as admittance is the inverse of the impedance $\left([\mathbf{Y}] = [\mathbf{Z}]^{-1}\right)$.

The mechanical impedance of the hand-arm is obtained using two specially designed handles. One has a cylindrical body and the other one has a shape that is as close as possible to the shape of the assembly handlebar. For each measurement, the handle is equipped with an accelerometer and is mounted on the 6 DOFs forces/moments sensor installed on the same excitation device as for the target measurements (Fig. 1.3). The same LMS system is used as a signal generator and the dynamic characteristics of the road are provided to the excitation system.

Measurements are performed with and without a hand on the handle. Because the handles are sufficiently rigid in the frequency range of interest, the handle impedance can then be subtracted from the total impedance (hand + handle) to obtain the hand-arm mechanical impedance [4, 9].

$$Z_{\text{Hand}}(\omega) = Z_{\text{Total}}(\omega) - Z_{\text{Handle}}(\omega) \tag{1.8}$$

The impedance data can then be inverted to get the mobility of the hand-arm system and used directly in Eq. (1.7).

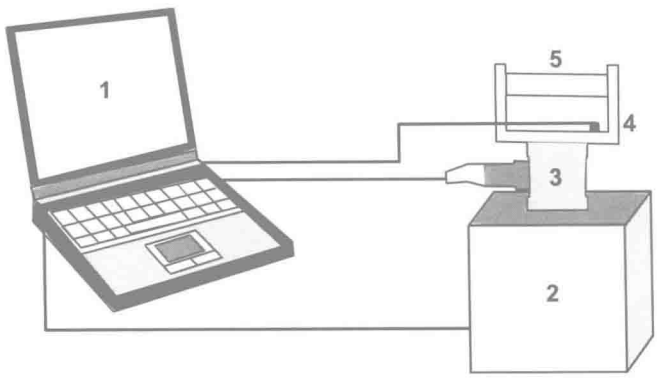

Fig. 1.3 Diagram of the hand-arm impedance measurement system (1: LMS Test.Lab 12A software, 2: Excitation device, 3: 6DOFs forces/moments sensor model MC3-A-500 from AMTI, 4: Accelerometer 356B11 type ICP from PCB Piezotronics, 5: Handle)

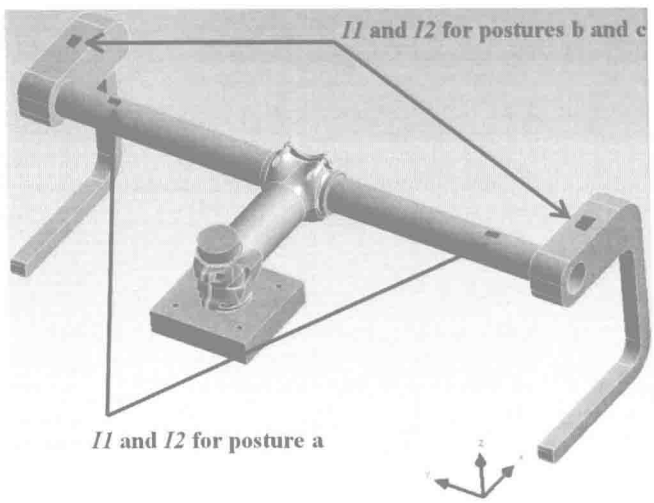

Fig. 1.4 Points location for the FE model of the assembly to obtain the needed FRFs for the different postures

The study is carried out on one subject to avoid inter-subject variability. The subject is asked to lean on the handle and to reproduce each posture to maintain the push forces along X and Z axes corresponding to the tested postures in the target measurements section. Since we are measuring each hand separately, we assume that the DC forces along X and Z axes should be half of the DC values retained when measuring on the structure assembly with both hands (target measurements).

1.2.3 Mechanical Structure Mobility

For the mechanical structure composed of a handlebar, a stem and a support, the FRFs needed for the FBS coupling process (Eq. 1.7) are obtained using an FE model (named FE FRFs). Translational DOFs (TDOFs) as well as rotational DOFs (RDOFs) are thus intrinsically available. This model of the mechanical assembly was previously updated to fit the experimental comparison in free – free conditions.

To perform the FBS coupling in Eq. (1.7), a total of 216 FE FRFs (TDOFs + RDOFs) are requested for the mechanical structure. These FRFs are obtained using the harmonic response section of the Ansys 14 Workbench software. The frequency resolution for the harmonic response of the structure is 1 Hz with a frequency span from 1 to 100 Hz. Moreover, specific commands need to be encoded to get rotational information at some points and to extract the results in *.txt files.

Considering the three different postures, the requested information in terms of FRFs are not the same for each one (Fig. 1.4)

FRFs for each posture are then computed. In Matlab, FE FRFs of the mechanical structure are coupled with experimental FRFs of both hand-arm dynamic characteristics to obtain an FBS prediction of the coupled structures.

1.3 Results

The FBS predictions for the hands coupled with the mechanical structure according to the three tested postures are compared to the target measurements corresponding to the hands holding the handlebar with the same postures and push forces. Comparisons are presented in terms of mobility along the Z-axis measured at the *I2* interface point corresponding to the right hand (Figs. 1.5, 1.6, and 1.7). In order to observe the influence of the hands touching the handlebar, the dynamic behavior of the mechanical structure alone is also shown (dotted line).

1.4 Discussion

Figures 1.5, 1.6, and 1.7 are presented with the same amplitude scale. It is possible to observe that the mobility of the structure alone at the point *I2* for posture a (Fig. 1.5) is lower than the mobility of the structure alone at the point *I2* for postures b and c (Figs. 1.6 and 1.7).

In terms of FBS prediction, the results for postures a and b (Figs. 1.5 and 1.6) demonstrate that the FBS model succeeds in providing reliable predictions for the influence of the hands on a mechanical structure with different postures and push forces applied by the subject on the structure. This is an indication that coupling between the hand-arm systems and a relatively complex mechanical structure is possible using this method.

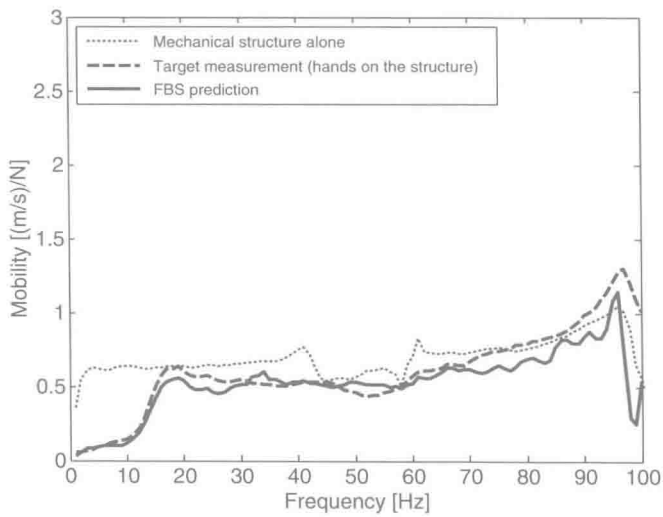

Fig. 1.5 Comparison between target measurement (hands on the structure) and FBS prediction for posture a

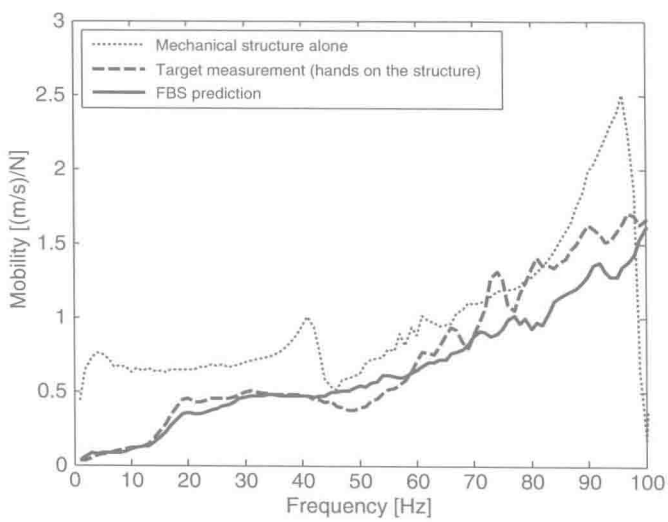

Fig. 1.6 Comparison between target measurement (hands on the structure) and FBS prediction for posture b

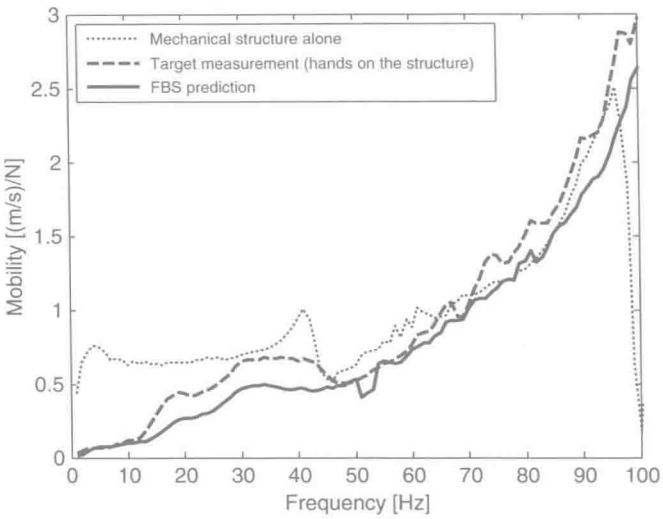

Fig. 1.7 Comparison between target measurement (hands on the structure) and FBS prediction for posture c

Nevertheless, results for posture c show some discrepancies (Fig. 1.7). The FBS model does not provide accurate results in the frequency span 1–50 Hz. This can be explained by the difficulty to reproduce the exact posture when measuring the dynamic characteristics of the hands separately. Furthermore, with such an extreme position of the wrists (see Fig. 1.2) there is an important contact surface between the hands and the mechanical structure. The hands were in contact at the two extremities of the handlebar but also with a part of the central tube while the FRFs from the FE model were obtained for a specific point. This alerts us to the fact that complex postures should be carefully reproduced during testing phases and also that the FE FRFs needed should be extracted for interface areas instead of interface points. The discrepancy between the FBS prediction and the target measurement for this specific posture may also be explained by the fact that, for hand measurement, only the vertical z-axis is considered in this work. This assumption could be too restrictive for the coupling of the hand-arm systems with the structure in this posture.

In terms of influence of the hands on the structure, we can easily identify that the posture of the subject has a clear influence on the dynamics of the assembly by looking at the target measurement of each figure from Figs. 1.5, 1.6, and 1.7. For example, with posture a, the subject provides a significant contribution to the structure dynamic up to 16 Hz while with posture b, the subject has a relatively important contribution up to 43 Hz. By integrating biodynamic measurements in the Frequency-Based Substructuring method, it is really important to control both the push force and the posture while carrying out measurements to obtain accurate predictions.

1.5 Conclusion

This study shows that reliable predictions can be obtained using the FBS method even with non-linear structures such as human body parts. Mechanical coupling predictions between the human body and a mechanical structure are thus possible using this method. Results show that it is important to control several parameters when performing the FBS coupling with a human body part because the mechanical behavior of the human body is sensitive to several factors such as position, orientation, and forces. This work also highlights the following merits of the FBS method: (1) Direct use of shaker test data, (2) Combination of substructures when only the data interfaces are known, (3) hybrid use of experimental and FE FRFs.

This work also highlights the possibility of predicting the influence of hand-arm systems on a structure using specific postures. The FBS method is a promising approach to study vibration interaction mechanisms between a mechanical structure and the human body. These results will be beneficial to further enhance interactions between humans and structures. This is a major breakthrough in human-structure interactions since it is possible to predict the influence of a human subject on a structure during the design phase of the structure in question. Limitations to this approach still remain due to the need to process a large amount of data and with regard to the computation time required for extracting FRFs.

Acknowledgements The authors gratefully acknowledge financial support from the National Science and Engineering Council of Canada (NSERC) and the participation of Cervélo and Vroomen – White Design.

References

1. Adewusi SA, Rakheja S, Marcotte P, Boileau P-E (2008) On the discrepancies in the reported human hand-arm impedance at higher frequencies. Int J Indust Ergon 38:703–714
2. Aldien Y, Marcotte P, Rakheja S, Boileau P-E (2006) Influence of hand-arm posture on biodynamic response of the human hand-arm exposed to z_h-axis vibration. Int J Ind Ergon 36:45–59
3. Aldien Y, Marcotte P, Rakheja S, Boileau P-E (2005) Mechanical impedance and absorbed power of hand-arm under x_h-axis vibration and role of hand forces and posture. Ind Health 43:495–508
4. Besa AJ, Valero FJ, Suñer JL, Carballeira J (2007) Characterization of the mechanical impedance of the human hand-arm system: the influence of vibration direction, hand-arm posture and muscle tension. Int J Ind Ergon 37:225–231
5. Burström L (1990) Measurements of the impedance of the hand and arm. Int Arch Occup Environ Health 62:431–439
6. Burström L (1997) The influence of biodynamic factors on the mechanical impedance of the hand and arm. Int Arch Occup Environ Health 69:437–446
7. Dong RG, Rakheja S, Schopper AW, Han B, Smutz WP (2001) Hand-transmitted vibration and biodynamic response of the human hand–arm: a critical review. Crit Rev Biomed Eng 29(4):391–441
8. Dong RG, Welcome DE, McDowell TW, Wu JZ (2008) Analysis of handle dynamics-induced errors in hand biodynamic measurements. J Sound Vib 318:1313–1333
9. Dong RG, Welcome DE, McDowell TW, Wu JZ (2006) Measurement of biodynamic response of human hand-arm system. J Sound Vib 294:807–827
10. Griffin MJ (1990) Handbook of human vibration. Academic, London
11. Griffin MJ, Whitham EM, Parsons KC (1982) Vibration and comfort, I. translational seat vibration. Ergonomics 25(7):603–630
12. International Standard Organization (ISO 2631) (1997) Mechanical vibration and shock—evaluation of human exposure to whole-body vibration. International Standard Organization
13. International Standard Organization (ISO/DIS 5349) (2001) Mechanical vibration—measurement and evaluation of human exposure to hand-transmitted vibration. International Standard Organization
14. Lundström R, Burström L (1989) Mechanical impedance of the human hand-arm system. Int J Ind Ergon 3:235–242
15. Marcotte P, Aldien Y, Boileau P-E, Rakheja S, Boutin J (2005) Effect of handle size and hand-handle contact force on the biodynamic response of the hand-arm system under z_h-axis vibration. J Sound Vib 283:1071–1091
16. Mansfield NJ (2005) Human response to vibration. CRC
17. Reynolds DD, Angevine EN (1977) Hand-arm vibration, Part II: vibration transmission characteristics of the hand and arm. J Sound Vib 51(2):255–265
18. Richard S (2005) Étude du comportement dynamique d'un vélo de route en lien avec le confort du cycliste. MScA Thesis, Université de Sherbrooke
19. Richard S, Champoux Y (2006) Development of a metric related to the dynamic comfort of a road bike. In: Proceedings of the IMAC XXIV, St. Louis, 2006
20. Avitabile P (2003) Twenty years of structural dynamic modification: a review. Sound Vib 14–25
21. Craig R, Bampton M (1968) Coupling of substructures for dynamic analysis. AIAA J 6(7):1313–1319
22. De Klerk D, Rixen D, De Jong J (2006) Frequency based substructuring (FBS) method reformulated according to the dual domain decomposition method. In: Proceedings of the fifteenth international modal analysis conference, Society for Experimental Mechanics, Paper 136, 2006
23. De Klerk D, Rixen DJ, Voormeeren SN, (2008) General framework for dynamic substructuring—history, review, and classification of techniques. AIAA J 46(5)
24. Ewins DJ (2000) Modal testing: theory, practice and application, 2nd edn. Research Studies Press
25. Hurty WC (1960) Vibrations of structural systems by component mode synthesis. J Eng Mech/Am Soc Civil Eng 86(4):51–69
26. Jetmundsen B (1986) On frequency domain methodologies for prescribed structural modification and subsystem synthesis. PhD Thesis, Rensselaer Polytechnic Institute, New York
27. Jetmundsen B, Bielawa R, Flanelly W (1988) Generalized frequency domain substructure synthesis. J Am Helicop Soc 33(1):55–65
28. Klosterman A (1971) On the experimental determination and use of modal representations of dynamic characteristics. Ph.D. Thesis, University of Cincinnati, Department of Mechanical Engineering
29. MacNeal R (1971) Hybrid method of component mode synthesis. Comput Struct 1(4):581–601
30. Mayes RL (2012) Tutorial on experimental dynamic substructuring using the transmission simulator method. In: Proceedings of the 30th international modal analysis conference. Society for experimental mechanics (Topics in experimental dynamics substructuring and wind turbine dynamics), pp 1–9
31. Perrier SS, Champoux Y, Drouet J-M (2012) Using substructuring to predict the human hand influence on a mechanical structure. In: Proceedings of the 30th international modal analysis conference. Society for Experimental Mechanics (Topics in experimental dynamics substructuring and wind turbine dynamics), pp 33–44
32. Lépine J, Champoux Y, Drouet J-M (2011) Excitation techniques for testing bike vibration transmission in the laboratory. In: Proceedings of the 29th International modal analysis conference. Society for experimental mechanics (Sensors, Instrumentation and Special Topics), p 35

Chapter 2
Investigation of Modal Iwan Models for Structures with Bolted Joints

Brandon J. Deaner, Matthew S. Allen, Michael J. Starr, and Daniel J. Segalman

Abstract Structures with mechanical joints are difficult to accurately model; even when the natural frequencies of the system remain essentially constant, the damping introduced by the joints is often observed to depend nonlinearly on amplitude. Although models for individual joints have been employed with some success, the modeling of a structure with many joints remains a significant obstacle. This work explores whether nonlinear damping can be applied in a modal framework, where instead of modeling each discrete joint within a structure, a nonlinear damping model is used for each mode of interest. This approach assumes that the mode shapes of the structure do not change significantly with amplitude and that there is negligible coupling between modes. The nonlinear Iwan joint model has had success in modeling the nonlinear damping of individual joints and is used as a modal damping model in this work. The proposed methodology is first evaluated by simulating a structure with a small number of discrete Iwan joints (bolted joints) in a finite element code. A modal Iwan model is fit to simulated measurements from this structure and the accuracy of the modal model is assessed. The methodology is then applied to actual experimental hardware with a similar configuration and a modal damping model is identified for the first few modes of the system. The proposed approach seems to capture the response of the system quite well in both cases, especially at low force levels when macro-slip does not occur.

Keywords Nonlinear damping • Bolted joints • Iwan model • Energy dissipation • Modal damping

2.1 Introduction

Mechanical joints are known to be a major source of damping in jointed structures. However, the physics at the interface are quite complex and the amplitude dependence of damping in mechanical joints has proven quite difficult to predict. For many systems, linear damping models seem to capture the response of a structure at calibrated force levels. However, that approach relies on testing the structure at large force levels to calibrate the model. Furthermore, that approach can be over conservative or even erroneous since a linear model does not capture the amplitude dependence of the damping. Thus, it is crucial to understand how mechanical joints behave at a range of force levels so that the response of a jointed structure can be modeled accurately.

In this work, nonlinearities associated with mechanical joints will be classified into two different regions, micro-slip and macro-slip. Consider the joint shown in Fig. 2.1, where a bolt is used to connect two slabs of material. The preload in the bolt creates a contact region between the two slabs near the bolt. If a force F is applied to the slabs, slip will occur at the

B.J. Deaner (✉) • M.S. Allen
Department of Engineering Physics, University of Wisconsin-Madison, 534 Engineering Research Building, 1500 Engineering Drive, Madison, WI 53706, USA
e-mail: bdeaner@wisc.edu; msallen@engr.wisc.edu

M.J. Starr
Component Science and Mechanics, Sandia National Laboratories, P.O. Box 5800, Albuquerque, New Mexico, 87185, USA
e-mail: mjstarr@sandia.gov

D.J. Segalman
Component Science and Mechanics, Sandia National Laboratories, P.O. Box 969, Mail Stop 9042, Livermore, California, 94551, USA
e-mail: djsegal@sandia.gov

R. Mayes et al. (eds.), *Topics in Experimental Dynamic Substructuring, Volume 2: Proceedings of the 31st IMAC, A Conference on Structural Dynamics, 2013*, Conference Proceedings of the Society for Experimental Mechanics Series 36,
DOI 10.1007/978-1-4614-6540-9_2,

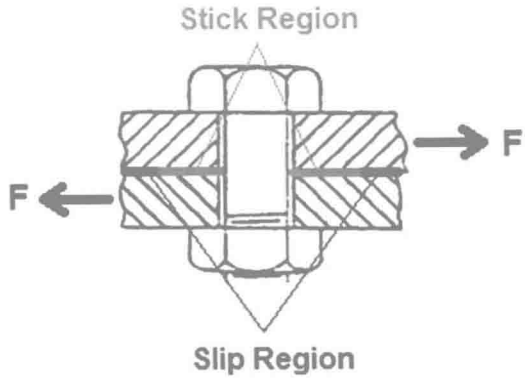

Fig. 2.1 Contact and Slip regions are shown for a mechanical joint undergoing micro-slip [1]

outskirts of the contact region. This means that there will be a region of stick and a region of slip as indicated in Fig. 2.1. For this case, the bolted joint is said to be undergoing micro-slip due to the small slip displacements that cause the frictional energy loss [1].

Macro-slip occurs when the stick region vanishes and larger slip displacements are possible. If a very large displacement is considered, the slabs of material will eventually come into contact with the bolt. This further complicates the system and is not considered in this work.

To capture the response of the joint in both the micro-slip and macro-slip regions, a 4-Parameter Iwan model was developed in [2]. This constitutive model has a small number of parameters and yet accounts for the key characteristics of the joint's response including the joint slip force (F_S), joint stiffness (K_T), and power law energy dissipation (χ, β). In the past decade, the 4-Parameter Iwan model has been implemented to predict the vibration of structures with a few discrete joints [3, 4]. However, when modeling individual joints, each joint requires a unique set of parameters $\{F_S, K_T, \chi, \beta\}$, which means that hundreds or even thousands of joint parameters may need to be deduced for the systems of interest. On the other hand, when a small number of modes are active in a response, some measurements have suggested that a simpler model may be adequate. Segalman investigated the idea of applying the 4-Parameter Iwan model in a modal framework in [5]. He used simulated measurements to deduce the modal Iwan parameters for two simple spring mass systems and compared this to the more rigorous approach where each discrete joint in the system was treated separately.

This work builds on Segalman's work [5] by simulating a more realistic finite element structure. First, a structure with four discrete Iwan joints is modeled using finite elements and the simulated response data is used to deduce a set of modal Iwan parameters. Particular attention is given to the degree to which the modal Iwan model captures the response of the finite element model that includes discrete Iwan joints. The methodology is then applied experimentally to an actual beam with a small link attached through two bolted joints. The beam was tested with free-free conditions, and great care had to be taken to assure that the suspension system did not dominate the measured damping. The initial results are promising, revealing that the modal Iwan approach does capture the response of the actual structure quite well in the micro-slip regime.

2.2 Nonlinear Energy Dissipation Model

The 4-Parameter Iwan model that is used in this work was initially presented in [2]. A historical review of the major contributors prior to Iwan's work led to the Iwan model being referred to as the Bauschinger-Prandtl-Ishlinskii-Iwan (BPII) model in a more recent work [6]. However, for simplicity and consistency with previous works, in this work the constitutive model will be referred to as the Iwan model.

2.2.1 Parallel–Series Iwan Model

A parallel arrangement of elements, each composed of a spring and frictional damper in series, is referred to as a parallel–series model in [7]. The physical representation of a parallel–series Iwan model is shown in [2]. The force in the joint, $F(t)$, is shown to have the following form,

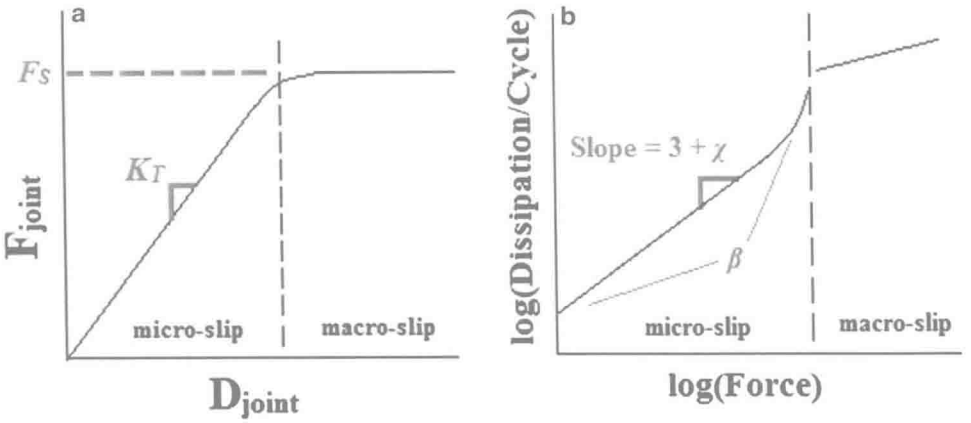

Fig. 2.2 (**a**) Both macro-slip force (F_S) and joint stiffness (K_T) can be found from the force-displacement relationship of the joint. (**b**) The χ value is found from the slope of the dissipation and the β value is a measure of dissipation level and shape of the dissipation curve

$$F(t) = \int_0^\infty \rho(\phi)\,[u(t) - x(t,\phi)]\,d\phi \tag{2.1}$$

where

$$\dot{x}(t,\phi) = \begin{cases} \dot{u} \text{ if } \|u - x(t,\phi)\| = \phi \text{ and } \dot{u}\,[u - x(t,\phi)] > 0 \\ 0 \text{ otherwise} \end{cases} \tag{2.2}$$

and $u(t)$ is the extension of the joint, $x(t,\phi)$ is the displacement of the frictional damper with strength ϕ and $\rho(\phi)$ is the population density of the spring and frictional damper elements with strength ϕ.

The response properties of the Iwan joint are characterized by the population density $\rho(\phi)$. Various population densities and their limitations are discussed in [6, 8]. Experiments at small force levels have revealed that the energy dissipated by the joint over one vibration cycle tends to be a power of the applied force. Analytically, the energy dissipation associated with pure material damping yields a power of 2.0, while the energy dissipation associated with friction between two bodies when the contact pressure is uniform yields a power of 3.0 [1, 2, 9, 10]. Experimentally, the dissipation tends to have a power-law slope that ranges between 2.0 and 3.0 [10]. One explanation for why experimental results often dissipate energy at a power less than 3.0 is due to the presumption that the contact pressure is nonuniformly distributed in joints [9].

In any event this means that at small force levels, a population density that dissipates energy in a power-law type fashion is desired. At large force levels, joints are known to exhibit a discontinuous nonlinearity associated with the initiation of macro-slip. This characteristic of joints must also be accounted for by the population density.

2.2.2 4-Parameter Iwan Model

To accommodate the behavior of joints at a large range of forces, a 4-parameter population density was developed in [2] with the form:

$$\rho(\phi) = R\phi^{\chi}\,[H(\phi) - H(\phi - \phi_{\max})] + S\delta(\phi - \phi_{\max}) \tag{2.3}$$

where $H(\,)$ is the Heaviside step function, $\delta(\,)$ is the Dirac delta function and the four parameters that characterize the joint include: R, which is associated with the level of energy dissipation, χ, which is directly related to the power law behavior of energy dissipation, $\phi_{\max}$, which is equal to the displacement at macro-slip, and the coefficient S, which accounts for a potential discontinuous slope of the force displacement plot when macro-slip occurs.

The four parameters $\{R, \chi, \phi_{\max}, S\}$ are converted to more physically meaningful variables $\{K_T, F_S, \chi, \beta\}$ in [2, 4]. F_S is the joint force necessary to initiate macro-slip, K_T is the stiffness of the joint, χ is directly related to the slope of the energy dissipation in the micro-slip regime, and β relates to the level of energy dissipation and the shape of the energy dissipation curve as the macro-slip force is approached.

This new set of parameters, $\{K_T, F_S, \chi, \beta\}$, can be deduced from the two plots seen in Fig. 2.2. Given a set of simulation or experimental data, there are a variety of methods that could be used to find the energy dissipation and joint force. A few of